Journal of Hydrology 559 (2018) 585–595

Contents lists available at ScienceDirect

Journal of Hydrology

journal homepage: www.elsevier.com/locate/jhydrol

Research papers

Applicability of Kinematic and Diffusive models for mud-flows: a steady state analysis

Cristiana Di Cristo [a], Michele Iervolino [b], Andrea Vacca [c,*]

[a] Dipartimento di Ingegneria Civile e Meccanica – Università di Cassino e del Lazio Meridionale, Via Di Biasio 43, 03043 Cassino, FR, Italy
[b] Dipartimento di Ingegneria Civile, Università degli Studi della Campania "Luigi Vanvitelli", Via Roma 29, 81031 Aversa, CE, Italy
[c] Dipartimento di Ingegneria Civile, Edile ed Ambientale, Università degli Studi di Napoli "Federico II", Via Claudio 21, 80125 Napoli, Italy

ARTICLE INFO

Article history:
Received 20 December 2017
Received in revised form 5 February 2018
Accepted 8 February 2018
Available online 24 February 2018
This manuscript was handled by Marco Borga, Editor-in-Chief, with the assistance of Marco Borga, Associate Editor

Keywords:
Mud-flow
Power-law fluid
Simplified wave models
Steady flow

ABSTRACT

The paper investigates the applicability of Kinematic and Diffusive Wave models for mud-flows with a power-law shear-thinning rheology. In analogy with a well-known approach for turbulent clear-water flows, the study compares the steady flow depth profiles predicted by approximated models with those of the Full Dynamic Wave one. For all the models and assuming an infinitely wide channel, the analytical solution of the flow depth profiles, in terms of hypergeometric functions, is derived. The accuracy of the approximated models is assessed by computing the average, along the channel length, of the errors, for several values of the Froude and kinematic wave numbers. Assuming the threshold value of the error equal to 5%, the applicability conditions of the two approximations have been individuated for several values of the power-law exponent, showing a crucial role of the rheology. The comparison with the clear-water results indicates that applicability criteria for clear-water flows do not apply to shear-thinning fluids, potentially leading to an incorrect use of approximated models if the rheology is not properly accounted for.

1. Introduction

In the geophysical context, a large number of flows, e.g. debris and/or mud flows, submarine or snow avalanches, is characterized by water transporting huge quantities of solids. These flows are often studied with the methods of fluid mechanics, combining appropriate flow schematizations with suitable rheological descriptions. A widespread approach considers a non-Newtonian rheology under purely viscous regime and a depth-integrated approximation.

For fluids with negligible yield stress, the power-law represents an effective rheological model for the description of the shear-thinning fine sediment-water mixtures which are often encountered in natural estuaries (e.g. Zhang et al. 2010) or in landsides (e.g. Carotenuto et al. 2015). Coupling the power-law rheology with the Von Karman approximation for the momentum conservation equation leads to the well-known shallow-layer model of Ng and Mei (1994). In several applications, some of the terms of the momentum conservation equation - i.e. inertia, pressure gradient, gravity and bottom shear stress – may be smaller than the others. In these circumstances, similarly to what is commonly exploited in open-channel flows in the context of flood routing, the flow model can be further simplified. For instance, neglecting the inertia terms leads to the so-called Diffusive Wave model, whereas the further disregarding of the pressure gradient term results in the Kinematic Wave approximation.

Even if efficient numerical methods for the solution of the complete momentum equations are currently available, the approximate models are still useful in the field of flood routing. In fact, in addition to the inherent benefit of reducing the computational effort, approximated wave models offer several further advantages. For instance, simplified models may be more easily coupled with high-resolution topographic data, and the boundary conditions more straightforwardly accounted for than in the full one (Aricò et al. 2011). Moreover, several studies showed a smaller sensitivity of simplified models to the errors in the topographic description with respect to the full one, demonstrating their accuracy and robustness to data uncertainty (Yu and Lane 2006; Weill et al. 2014; Aricò et al. 2016).

Most of these advantages do not depend on the flowing medium, so it does not surprise that simplified models have been widely used also with non-Newtonian fluids, to reproduce either the results of laboratory experiments (Huang and Garcia 1998; Balmforth et al. 2007; Ancey and Cochard 2009; Pudasaini, 2001; Ancey et al. 2012) or mud/debris flows occurred in the field.

* Corresponding author.
E-mail address: vacca@unina.it (A. Vacca).

https://doi.org/10.1016/j.jhydrol.2018.02.016
0022-1694/

O'Brien et al. (1993) developed the FLO-2D code for mud/debris flow simulations, including both Diffusive and Kinematic approximations. Arattano and Savage (1994) simulated the two debris flows occurred in 1981 on Mount St. Helens, Washington, U.S.A. with a model based on Kinematic approximation, obtaining a good agreement with the field data. Arattano et al. (2006), in simulating the debris flow occurred in 2004 in an experimental basin on the Italian Alps, showed that the Kinematic approximation, based on the rheological model by Honda and Egashira (1997), was able to fairly reproduce the recorded hydrographs. Arattano and Franzi (2010) analyzed the applicability of both Diffusive and Kinematic Wave models for reproducing debris flow occurred in an Italian instrumented torrent, evaluating in a real-case scenario the actual magnitude of the neglected terms. Chiang et al. (2012) studied landslides and debris flows caused by Morakot typhoon in Taiwan on August 2009, by means of a cell model with a Kinematic approximation of the flow model, achieving a predictive capability of the affected area and of the deposition volume. Rengers et al. (2016) investigated post-wildfire debris flows adopting the kinematic approximation. It has been shown that the Kinematic Wave model represents a suitable approach for predicting flood and debris flows timing in steep, burned watersheds. Gregoretti et al. (2016) applied an approach similar to Chiang et al. (2012) for the simulation of the debris flow on the Rio Lazer (Dolomites, North-Eastern Italian Alps), obtaining a good agreement between computed and observed results in terms of debris-flow deposition area and changes in valley morphology.

The promising results achieved in the above applications open a wider question on a more general definition of the applicability range of simplified models. This aspect has been widely studied in the literature for clear-water open-channel flows in turbulent regime, and three approaches to assess the applicability of approximated models have been followed. The first technique consists in analysing the linearized version of both the complete and the approximated models and comparing the properties of the resulting unsteady solutions as a function of the dimensionless wave period (Ponce et al. 1978; Menendez and Norscini, 1982; Dooge et al. 1987; Lamberti and Pilati 1996; Singh 1996; Tsai 2003). The other two methods account for the non-linearity of the flow model. Indeed, the second approach is essentially based on the estimation of the magnitude of the terms neglected in the momentum equation (Woolhiser and Liggett 1967; Morris and Woolhiser 1980; Fread 1983; Ferrick 1985; Moussa and Boequillon, 1996; Moramarco and Singh 2000; Perumal and Sahoo 2007). Finally, the third approach relies on the solution of the full and the approximated models and on the analysis of the differences among the results. Either steady (Govindaraju et al. 1988a,b; Parlange et al. 1990; Singh and Aravamuthan 1995a,b, 1996; Moramarco et al. 2008a) or unsteady (Moramarco et al. 2008b) flow conditions have been investigated and an estimation of the spatial (resp. temporal) error resulting from to the application of the approximated models has been provided. Some of these criteria have been validated through the comparison with the dynamics of recorded flood events (Moramarco et al. 2008b).

As far as non-Newtonian fluids are concerned, Di Cristo et al. (2014a,b) followed the first of the above approaches in order to define applicability criteria for some approximate models for mud floods, considering a Herschel & Bulkley and a power-law rheology, respectively. In an unbounded channel, a linearized version of the flow model, valid in the neighbourhood of uniform condition, has been considered. The expressions of celerity and attenuation factor of the primary wave for the full and some simplified (i.e. kinematic, diffusion and quasi-steady) models have been compared. Considering an accuracy threshold of 95%, applicability criteria have been deduced in terms of the dimensionless wave period of the flow perturbation, which can be related the dimensionless rising time of the flood hydrograph. Di Cristo et al. (2017) addressed the same problem of Di Cristo et al. (2014b) but for finite-length channels. The analysis, based on the evaluation of three shape factors of the linearized upstream channel response function, has shown that the diffusive approximation provides the best performance, especially for low values of the Froude number. Despite they natively account for the power-law rheology, both Di Cristo et al. (2014b) and Di Cristo et al. (2017) studies deal with linearized flow models.

The present paper investigates the applicability of Kinematic and Diffusive Wave models in presence of power-law fluids, fully accounting for the non-linearity of governing equations. Steady state conditions are considered, extending to the shear-thinning power-law rheology the analyses previously performed for turbulent clear-water flows (Govindaraju et al. 1988a,b; Parlange et al. 1990; Singh and Aravamuthan 1995a,b, 1996; Moramarco et al. 2008a, de Almeida and Bates 2013). As for the turbulent clear-water case (Moramarco et al. 2008a), the analysis considers accelerated hypocritical flow profiles in mild slope channel with the critical depth assigned as the downstream boundary condition. Applicability criteria for approximated models in finite-length channels are sought for. To this aim, the analytical solution of the flow depth profiles of both Full and Approximated models, in an infinitely wide channel, has been derived. Based on the theoretical developments, the spatial distribution of the error for the approximated models has been analyzed, as a function of the fluid rheology. Assuming a threshold of 5% for the channel-length-averaged error, the applicability conditions have been individuated in terms of the governing dimensionless parameters, i.e. kinematic wave and Froude numbers, for several values of the power-law exponent.

The outline of the paper is as follows: Section 2 reports the governing equations for the Full Wave, Diffusive Wave and Kinematic Wave models, while in Section 3 the analytical solutions for steady-state flow profiles are derived. Section 4 presents the results relative to the comparison of the Full with both the Kinematic and Diffusive approximations and the resulting applicability criteria. Finally, conclusions are drawn in Section 5.

2. Governing equations

Let us consider a homogeneous layer of a shear-thinning power-law fluid flowing over a fixed bed, with a constant inclination (θ) with respect to the horizontal plane, without lateral inflow or outflow. The fluid is regarded as incompressible. Assuming that:

- spatial variations occur over scales larger than the flow depth;
- flow resistance by the sidewalls is negligible with respect to that by the bottom;
- surface tension is negligible;

the dimensional depth-averaged momentum and mass conservation equations are (Di Cristo et al. 2017):

$$\frac{\partial \tilde{u}\tilde{h}}{\partial \tilde{t}} + \beta \frac{\partial \tilde{h}\tilde{u}^2}{\partial \tilde{x}} + g\tilde{h}\frac{\partial \tilde{h}}{\partial \tilde{x}}\cos\theta - g\tilde{h}\sin\theta + \frac{\tilde{\tau}_b}{\rho} = 0 \tag{1}$$

$$\frac{\partial \tilde{h}}{\partial \tilde{t}} + \frac{\partial \tilde{u}\tilde{h}}{\partial \tilde{x}} = 0 \tag{2}$$

in which $\tilde{t}$ is the time, $\tilde{x}$ the streamwise coordinate, g and ρ the gravity and the fluid density respectively, $\tilde{h}$ the flow depth, $\tilde{u}$ the depth-averaged velocity, β the momentum correction factor and

$\tilde{\tau}_b$ the bottom shear stress. The terms in Eq. (1) represent, in the order, the contributions of local (I) and convective (II) inertia, pressure gradient (III), gravity (IV), friction (V).

Considering the flow in laminar regime, the power-law model proposed by Ng and Mei (1994) is adopted. As described in Appendix A, the expressions of the momentum correction factor and of the bottom stress are:

$$\beta = 2\frac{2n+1}{3n+2} > 1 \tag{3}$$

$$\tilde{\tau}_b = \mu_n\left(\frac{2n+1}{n}\frac{\tilde{u}}{\tilde{h}}\right)^n \tag{4}$$

In (3), (4) μ_n and n denote the consistency and the rheological index, respectively. The rheological index ranges between 0 and 1 for a shear-thinning fluid, whereas values larger than 1 represent shear-thickening behavior. For a given flow rate $\tilde{q}$ (for unit width), the following dimensionless quantities are introduced:

$$x = \tilde{x}/\tilde{L}, \quad t = \tilde{t}\tilde{u}_N/\tilde{L}, \quad u = \tilde{u}/\tilde{u}_N, \quad h = \tilde{h}/\tilde{h}_N, \quad \tau_b = \tilde{\tau}_b/\tilde{\tau}_{b,N} \tag{5}$$

where the subscript N denotes the normal, i.e. uniform, flow variables corresponding to $\tilde{q}$ and $\tilde{L}$ is the dimensional channel length. Therefore, the dimensionless form of the flow equations (1), (2) is:

$$\frac{\partial hu}{\partial t} + \beta\frac{\partial hu^2}{\partial x} + \frac{h}{F_N^2}\frac{\partial h}{\partial x} + Kh\left(\frac{\tau_b}{h} - 1\right) = 0 \tag{6}$$

$$\frac{\partial h}{\partial t} + \frac{\partial uh}{\partial x} = 0 \tag{7}$$

with

$$\tau_b = \left(\frac{u}{h}\right)^n \tag{8}$$

In Eq. (6) the governing parameters are the normal Froude number, F_N, and the kinematic wave number, K, expressed by:

$$F_N = \frac{\tilde{u}_N}{\sqrt{g\tilde{h}_N\cos\theta}}, \qquad K = \frac{1}{F_N^2}\frac{\tilde{L}}{\tilde{h}_N}\tan\theta \tag{9}$$

In steady flow conditions, denoted with subscript S, Eqs. (6) and (7), accounting for Eq. (8), reduce to the following system:

$$(2\beta-1)u_S\frac{\mathrm{d}u_S}{\mathrm{d}x} + \left[(\beta-1)\frac{u_S^2}{h_S} + \frac{1}{F_N^2}\right]\frac{\mathrm{d}h_S}{\mathrm{d}x} = K\left(1 - \frac{u_S^n}{h_S^{n+1}}\right) \tag{10}$$

$$\frac{\mathrm{d}}{\mathrm{d}x}(u_S h_S) = 0 \tag{11}$$

which may be rewritten in terms of flow depth only, as follows:

$$\frac{\mathrm{d}h_{S,FM}}{\mathrm{d}x} = \frac{KF_N^2}{h_{S,FM}^{2(n-1)}}\frac{h_{S,FM}^{2n+1} - 1}{h_{S,FM}^3 - \beta F_N^2} \tag{12}$$

Eq. (12), representing the steady formulation of the Full Wave Model (FWM), puts in evidence that, similarly to the Turbulent Clear-Water (TCW) case (Govindaraju et al. 1988a,b; Moramarco et al. 2008a) even for the power-law fluids, the flow depth profile depends only on F_N and K, along with the boundary condition. In what follows, similarly to the TCW case (Moramarco et al. 2008a) one of the two pairs (F_N, K) or $(F_N, \hat{K})$, with $\hat{K} = KF_N^2 = \tilde{L}/\tilde{h}_N\tan\theta$, will be considered.

The Diffusive Wave Model (DWM) comes from Eq. (10) neglecting the convective acceleration (i.e. the first term), therefore the counterpart of Eq. (12) reads:

$$\frac{\mathrm{d}h_{S,DWM}}{\mathrm{d}x} = KF_N^2\frac{h_{S,DWM}^{2n+1} - 1}{h_{S,DWM}^{2n+1}} \tag{13}$$

The steady formulation of the Kinematic Wave Model (KWM), which disregards in Eq. (10) also the pressure gradient term, leads to the following simple equation:

$$h_{S,KWM} = 1 \tag{14}$$

3. Solution of the steady flow depth profile

In order to quantify the errors of the approximated models, the solution of Eqs. (12)–(14) is needed. While this is trivial for the KWM (see Eq. (14)), the steady flow depth profile predicted by both Full and Diffusive Wave models has to be evaluated from the integration of the non-linear ordinary differential equations (12) and (13), respectively. In the present paper, a closed form solution has been derived. To this aim, as far as the FWM is concerned, from the integration of Eq. (12) it follows:

$$x - const = \frac{1}{KF_N^2}\left[\int\frac{h^{2n+1}}{h^{2n+1}-1}\mathrm{d}h - \beta F_N^2\int\frac{h^{2(n-1)}}{h^{2n+1}-1}\mathrm{d}h\right] \tag{15}$$

In Eq. (15) the subscript S has been dropped for the sake of simplicity. The r.h.s. of Eq. (15) is then rewritten as follows

$$-\frac{w}{KF_N^2}\left[\int\frac{\xi^w}{1-\xi}\mathrm{d}\xi - \beta F_N^2\int\frac{\xi^{-2w}}{1-\xi}\mathrm{d}\xi\right] \tag{16}$$

with

$$w = \frac{1}{2n+1}, \xi = h^{2n+1} \tag{17}$$

Accounting for the Chebyshev integral identity (Weisstein, 1998):

$$\int x^p(1-x)^q\mathrm{d}x = \frac{x^{1+p}\mathrm{F}(p+1,-q;p+2;x)}{1+p} \tag{18}$$

F(a,b;c;z) being the hypergeometric function, the closed form solution of Eq. (15) reads:

$$x = -\frac{1}{KF_N^2}\left[\frac{h^{2n+2}}{2(n+1)}\mathrm{F}\left(\frac{2n+2}{2n+1},1;\frac{4n+3}{2n+1};h^{2n+1}\right) + \beta F_N^2\frac{h^{2n-1}}{2n-1}\mathrm{F}\left(\frac{2n-1}{2n+1},1;\frac{4n}{2n+1};h^{2n+1}\right)\right] + const \tag{19}$$

With reference to hypocritical currents and imposing that for $x = 0$ a known flow depth (h_*) is prescribed, the flow depth profile, for $-1 \leqslant x_{FM} \leqslant 0$, may be deduced through the following implicit equation:

$$x_{FM} = \frac{\beta F_N^2}{2(n+1)(2n-1)K}\left[2h^{2n-1}(1+n)\mathrm{F}\left(\frac{2n-1}{2n+1},1;\frac{4n}{2n+1};h^{2n+1}\right) - 2h_*^{2n-1}(1+n)\mathrm{F}\left(\frac{2n-1}{2n+1},1;\frac{4n}{2n+1};h_*^{2n+1}\right)\right] + \frac{1}{KF_N^2}\frac{1}{2(n+1)(2n-1)}\left[h^{2n+2}(1-2n)\mathrm{F}\left(\frac{2n+2}{2n+1},1;\frac{4n+3}{2n+1};h^{2n+1}\right) - h_*^{2n-1}(1-2n)\mathrm{F}\left(\frac{2n+2}{2n+1},1;\frac{4n+3}{2n+1};h_*^{2n+1}\right)\right] \tag{20}$$

Solution (20) holds for all positive n values except $n = 1/2$. For such a value of the power-law exponent, the following expression holds (Appendix B):

$$x_{FM} = \frac{1}{KF_N^2}\left[h - h_* + \frac{1-\beta F_N^2}{2}\ln\left(\frac{h-1}{h_*-1}\right) - \frac{1+\beta F_N^2}{2}\ln\left(\frac{h+1}{h_*+1}\right) + \beta F_N^2 \ln\left(\frac{h}{h_*}\right)\right] \tag{21}$$

Eqs. (20) and (21) allow to compute the flow depth profile of steady flow of a power-law fluid, showing that the hypergeometric functions, commonly employed in the context of turbulent clear-water flows (Chyan-Deng 2014), may be fruitfully used even dealing with different rheologies.

Starting from Eqs. (20) and (21) and taking the limit for $\beta F_N^2 \to 0$ its easy to verify that the counterparts of (20) and (21) for the Diffusive Wave model read:

$$x_{DWM} = \frac{1}{2(n+1)(2n-1)KF_N^2}\left[h^{2n+2}(1-2n)\mathrm{F}\left(\frac{2n+2}{2n+1},1;\frac{4n+3}{2n+1};h^{2n+1}\right) - h_*^{2n-1}(1-2n)\mathrm{F}\left(\frac{2n+2}{2n+1},1;\frac{4n+3}{2n+1};h_*^{2n+1}\right)\right] \tag{22}$$

$$x_{DWM} = \frac{1}{KF_N^2}\left\{h - h_* + \frac{1}{2}\left[\ln\left(\frac{h-1}{h_*-1}\right) - \ln\left(\frac{h+1}{h_*+1}\right)\right]\right\} \tag{23}$$

For the sake of clarity, Figures 2 and 3 report the calculated accelerated flow depth profiles for two different Froude numbers values (namely, Fig. 2: $F_N = 0.1$; Fig. 3: $F_N = 0.5$) in a mild slope channel, i.e. $F_N < F_{N,c}$, $F_{N,c} = 1/\sqrt{\beta}$ being the critical Froude number (Campomaggiore et al. 2016). Both the Full and Diffusive Wave models have been considered. Three different n values, namely n = 0.25, 0.5, 1.0, have been selected, while the kinematic wave number (K) has been fixed equal to 5. At the downstream end of the channel ($x = 0$), critical flow depth $h_c = \sqrt[3]{\beta F_N^2}$ (Campomaggiore et al. 2016) has been imposed. For the considered power-law exponent values, Fig. 1 depicts the critical flow depth as a function of the Froude number.

Figure 1 puts in evidence that, owing to the dependence of the momentum correction factor on the power-law exponent (Eq. (3)), the critical flow depth increases with n, for a fixed value of Froude number. Moreover, it is also easy to verify that the critical Froude number $F_{N,c}$ reduces with the power-law exponent, reaching the minimum value ($F_{N,c}^{\min} = 0.913$) for $n = 1$.

Figures 2 and 3 indicate that, independently of the Froude number, the power-law exponent strongly influences the flow depth profiles, for both models. The increase of the power-law exponent leads to a growth of the flow depth gradient, for both models. Therefore, a careful rheological characterization of the flow medium appears to be mandatory for a correct prediction of the accelerated flow depth profiles.

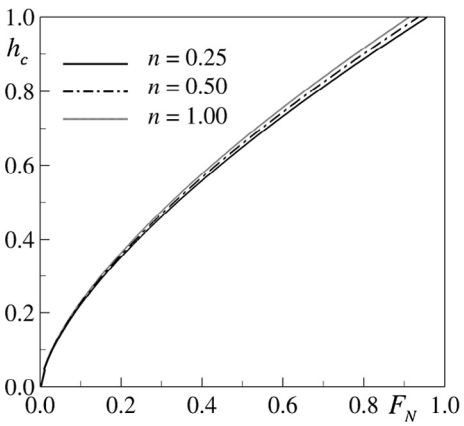

Fig. 1. Critical flow depth as a function of the Froude number.

4. Results

Based on the above closed forms of the steady flow depth profiles, the present section compares the results of the approximated models, i.e. KWM and DWM, with those of the FWM. To this aim, for a fixed value of the power-law exponent and of the (F_N, K) pair, for both Approximated Wave Models (AWM) the spatial distribution of the relative error is evaluated as:

$$\varepsilon_{AWM}(x) = \frac{h_{AWM}(x) - h_{FWM}(x)}{h_{FWM}(x)} \tag{24}$$

Following Moramarco et al. (2008a), the analysis has been carried out referring to accelerated hypocritical currents in a mild slope channel and assuming as downstream boundary condition the critical flow depth. In this condition, the largest errors in the application of the approximated models are expected (Moramarco et al., 2008a). In what follows, for the sake of comparison, the results concerning the turbulent clear water (TCW) case, with the Manning resistance formula, are also discussed. The closed form of the flow depth profile for this case can be found, for instance, in (Chyan-Deng, 2014).

Figure 4 depicts the spatial distribution of the relative error as far as the KWM is concerned (ε_{KWM}), for K = 3, 5, 10, 30. Three different n values have been considered, namely n = 0.25 (Fig. 4a), n = 0.5 (Fig. 4b), n = 1.0 (Fig. 4c), along with the turbulent clear water case (TCW: Fig. 4d). The Froude number has been fixed equal to 0.1.

Similarly to the turbulent clear-water case (Fig. 4d), for all n values, Fig. 4a, b, c show that, independently of the K value, ε_{KWM} increases monotonically with the channel abscissa x and decreases with K. For all the values of the kinematic wave number, ε_{KWM} reduces with n. The comparison with the turbulent clear-water case (Fig. 4d) puts in evidence that the performances of the Kinematic Wave model significantly depend on the rheology of the flowing medium: both a pronounced shear-thinning attitude and a small value of the kinematic wave number induce an increase of ε_{KWM} for a power-law fluid with respect to ε_{KWM}^{TCW}. For instance, for K = 3, at x = −0.5, the TCW model predicts $\varepsilon_{KWM}^{TCW} = 0.84$, whereas $\varepsilon_{KWM}^{n=0.5} = 1.76$. Therefore, migrating the evaluations for TCW to a shear-thinning power-law fluid could imply a strong underestimation of the error associated to the KWM model.

Figure 5 depicts the ε_{DWM} spatial distribution along the channel for the same K and n values of Fig. 4, while Figs. 6 and 7 represent the counterparts of Figs. 4 and 5 for F_N = 0.5.

Figure 5 shows that for all the considered values of power-law exponent and kinematic wave number, the magnitude of the ε_{DWM} is much smaller than the one of the KWM. Moreover, owing to the fulfillment of the downstream boundary condition and differently from the KWM, ε_{DWM} is a non-monotone function along the channel. Even though all the considered cases show a similar trend, the abscissa of the maximum value of $|\varepsilon_{DWM}|$ depends on both K and n values. An increase of both K and n values shifts downstream the $|\varepsilon_{DWM}|$ maximum location.

The comparison of Fig. 5a, b, c with Fig. 5d suggests that even in applying the DWM model, the results deduced for TCW cannot be safely applied for the power-law fluids, especially for small values of n. Comparing Fig. 5c and Fig. 5d it follows that, independently of the K value, although very close to the outlet ε_{DWM}^{TCW} overwhelms the corresponding one for the power-law fluid, in most of the channel $\varepsilon_{DWM}^{TCW}/\varepsilon_{DWM}^{n=0.5}$ is smaller than 0.5. Therefore, similarly to the Kine-

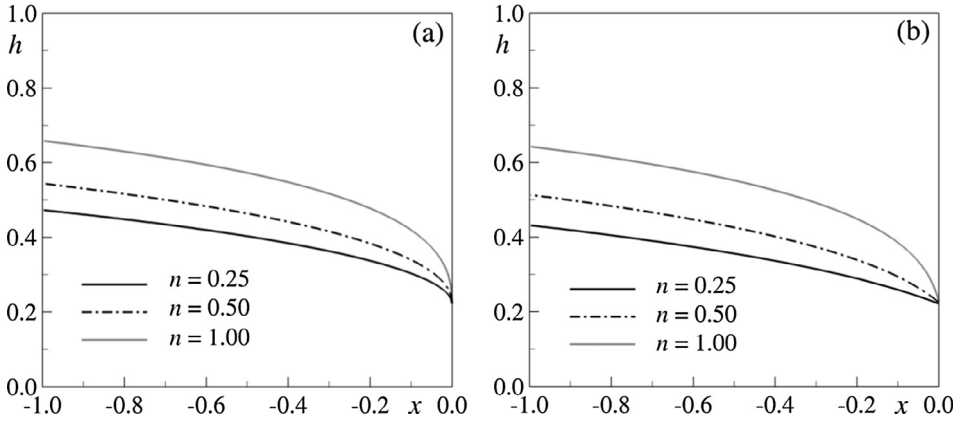

Fig. 2. Flow depth profiles: $F_N = 0.1$, $K = 5$. (a) FWM; (b) DWM.

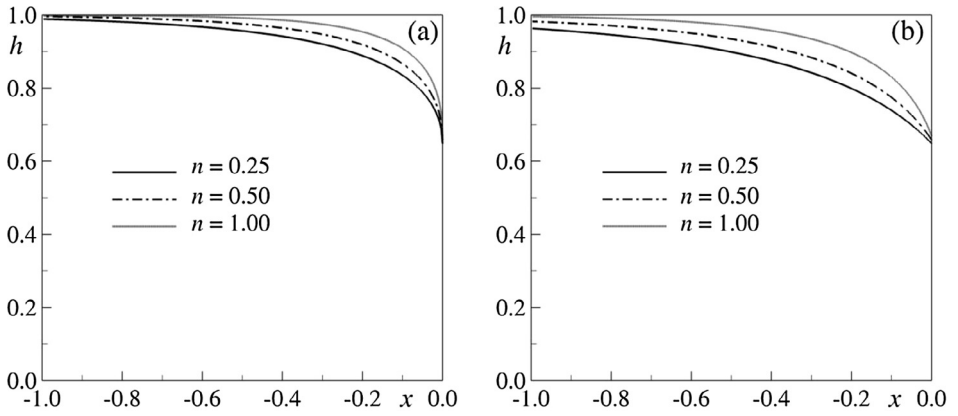

Fig. 3. Flow depth profiles: $F_N = 0.5$, $K = 5$. (a) FWM; (b) DWM.

matic Wave model, it is expected that the bounds for a correct application of the DWM in the presence of a power-law fluid may significantly differ from those deduced for the TCW case.

Figures 6 and 7, representing the counterparts of Figs. 4 and 5 for $F_N = 0.5$, show that an increase of the Froude number leads a reduction, for all n and K values, of both ε_{KWM} and ε_{DWM} values, although confirming the general trend suggested by the $F_N = 0.1$ case.

An overall analysis of the accuracy of the Approximated Wave models may be carried out considering the magnitude of the average of the error along the channel (Moramarco et al. 2008a) ε^*_{AWM}. For the KWM model the average was computed for $-0.95 \leqslant x \leqslant -0.05$, i.e. considering the part of the channel less influenced by the boundary conditions (Singh and Aravamuthan 1997; Moramarco et al. 2008a). Figures 8 and 9 depict, for two Froude numbers, namely F_N=0.1 and F_N=0.5, the averaged error ε^*_{AWM} as function of the dimensionless parameter $\hat{K}$. Again the n = 0.25, 0.5, 1.0 values, along with the TCW case, have been considered for both approximated models (ε^*_{KWM} Figs. 8a and 9a; ε^*_{DWM} Figs. 8b and 9b).

Figures 8a and 9 put in evidence that, independently of n values and similarly to the TCW case, ε^*_{KWM} curves overwhelm the corresponding ones of the Diffusive Wave model (in the $F_N = 0.1$ case even of an order of magnitude) and, for both models, the error reduces when the power-law exponent increases. For $F_N = 0.1$ Fig. 8a and Fig. 8b show a monotonically decreasing behavior with $\hat{K}$. Moreover, they suggest that, in averaged sense, the results pertaining to the turbulent clear-water case may be applicable even for the laminar case, i.e. $n = 1$, especially for the KWM. Figure 9 indicates that an increase of the Froude number has a different effect on the two approximated models. In fact, for a fixed $\hat{K}$ value, ε^*_{KWM} decreases from the $F_N = 0.1$ to the $F_N = 0.5$ case, while ε^*_{DWM} increases. Furthermore, Fig. 9a hints the same monotone decrease of the error with $\hat{K}$, while for the DWM Fig. 9b reveals for very small values of $\hat{K}$ an increasing trend reaching a peak value and then the usual decreasing behavior. Finally, it is also confirmed that even for F_N=0.5, the turbulent and laminar clear-water flows have similar results, especially for the KWM.

The results of Figs. 8 and 9 imply that it is possible to individuate a lower bound of the kinematic wave number $\hat{K}_{LB}$, above which the Approximate Wave Model is applicable with a prescribed accuracy. Assuming as applicability condition $\varepsilon^*_{AWM} \leqslant 5\%$ (Moramarco et al., 2008a), for each n value, the applicability map in the plane ($\hat{K}$, F_N) may be deduced for both Kinematic (Fig. 10a) and Diffusive (Fig. 10b) Wave Models.

Figure 10a clearly shows that, for all n values, the lower bound ($\hat{K}_{LB}$) above which the KWM is applicable, monotonically decreases when the Froude number increases, as observed also for the TCW case. Moreover, a decrease of the power-law exponent reduces the extension of the applicability region. Differently, Fig. 10b indicates that, as far as the DWM is concerned and similarly to the TCW flow, the lower bound $\hat{K}_{LB}$ is not a monotone function of F_N even for the power-law fluids. Also in this case, a reduction in terms of power-law exponent induces a restriction of the applicability region of the DWM.

Figure 10 points out that, for each value of the power-law exponent, it exists a threshold value $\hat{K}_{TV} = \max_{F_N} \hat{K}_{LB}$, which may be con-

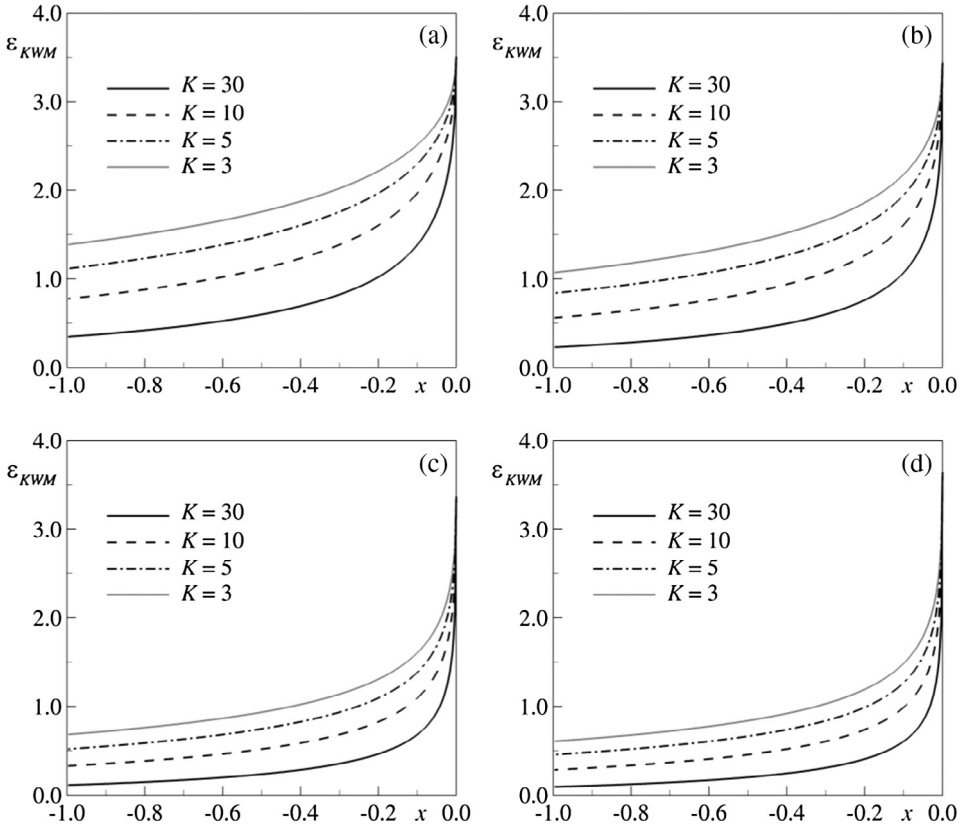

Fig. 4. Spatial distribution of the relative error of the KWM (F_N = 0.1): (a): n = 0.25; (b): n = 0.5; (c): n = 1.0; (d): TCW.

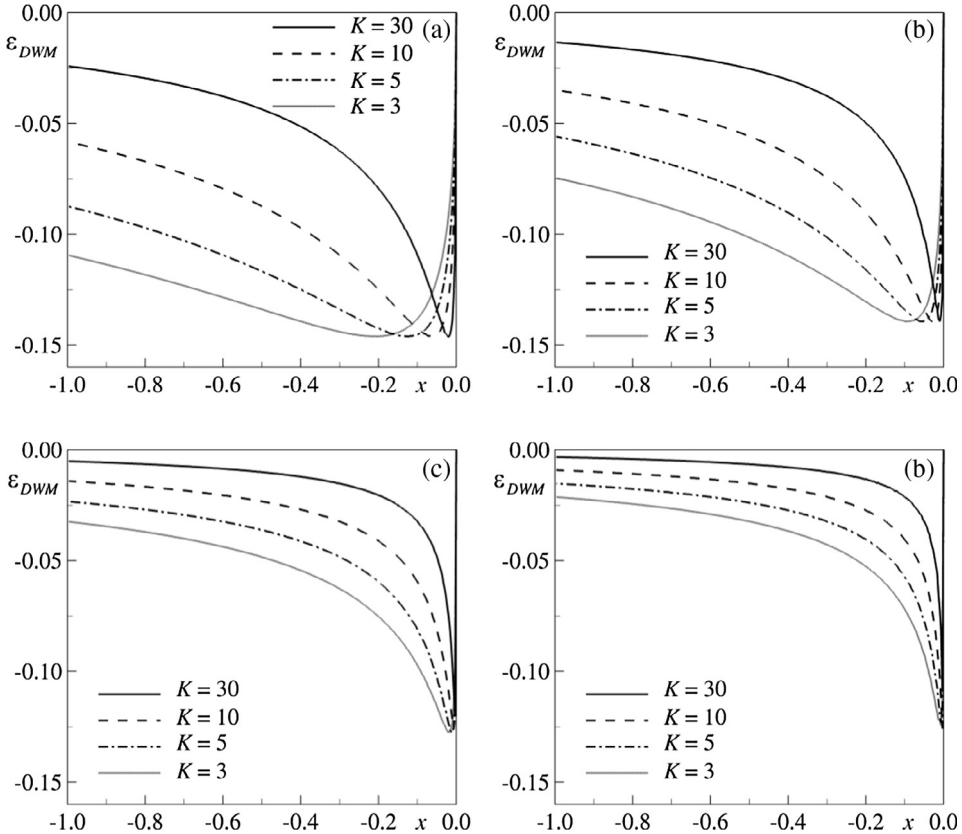

Fig. 5. Spatial distribution of the relative error of the DWM (F_N = 0.1): (a): n = 0.25; (b): n = 0.5; (c): n = 1.0; (d): TCW.

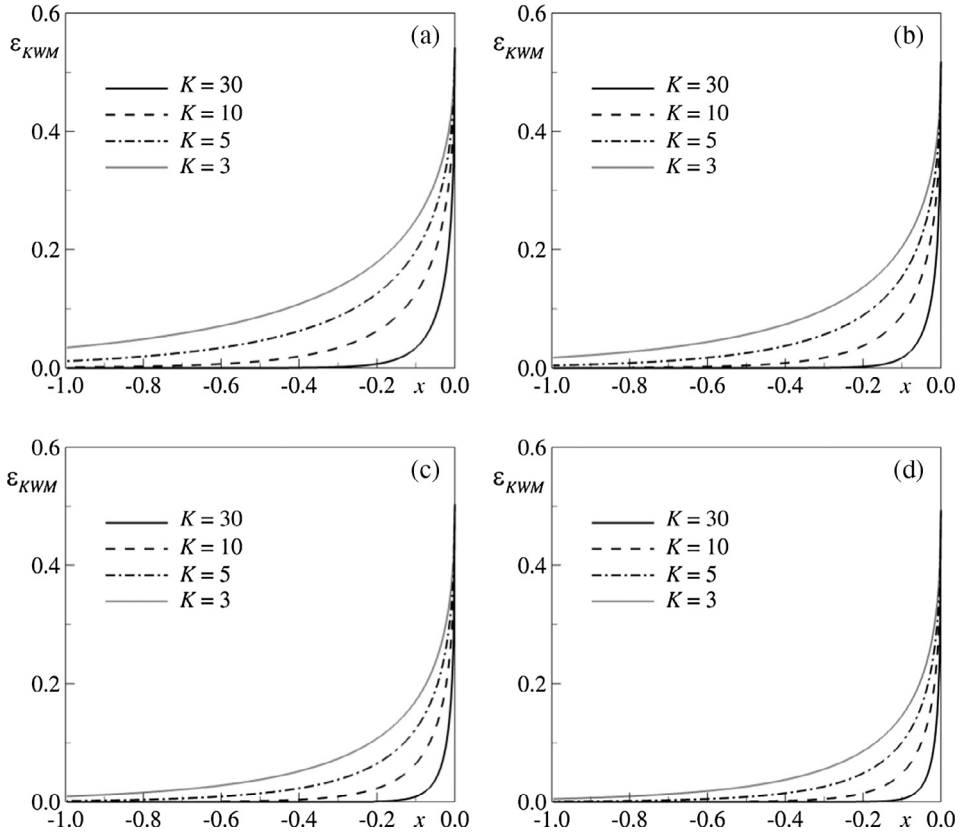

Fig. 6. Spatial distribution of the relative error of the KWM ($F_N = 0.5$): (a): $n = 0.25$; (b): $n = 0.5$; (c): $n = 1.0$; (d): TCW.

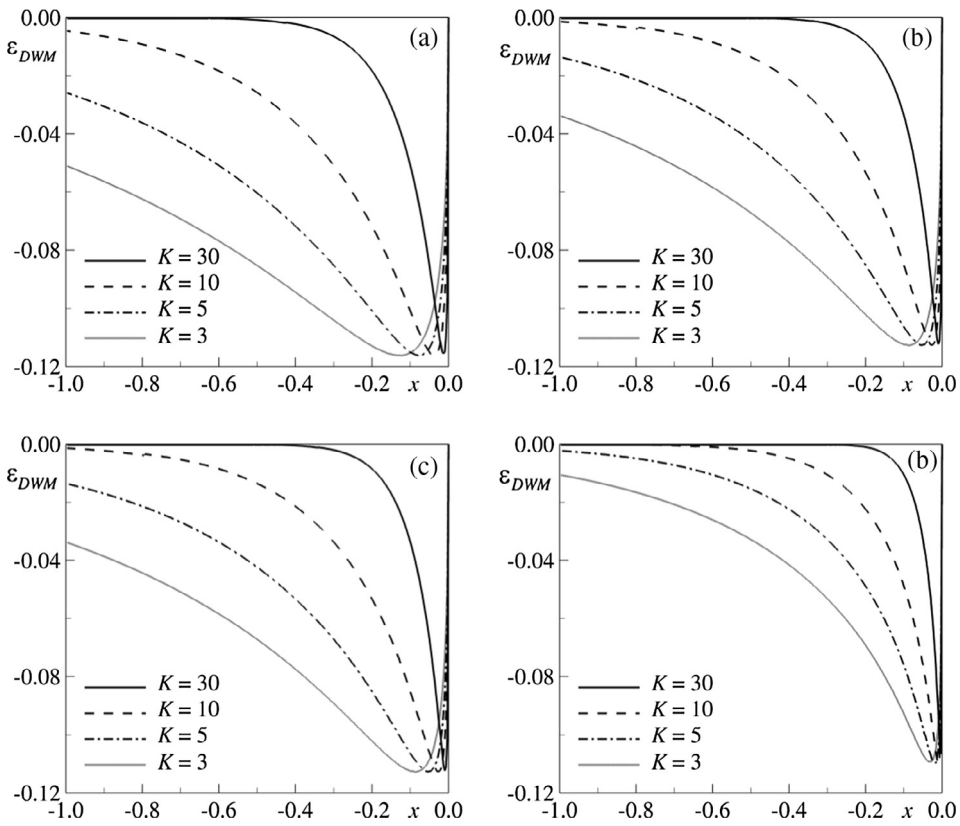

Fig. 7. Spatial distribution of the relative error of the DWM ($F_N = 0.5$): (a): $n = 0.25$; (b): $n = 0.5$; (c): $n = 1.0$; (d): TCW.

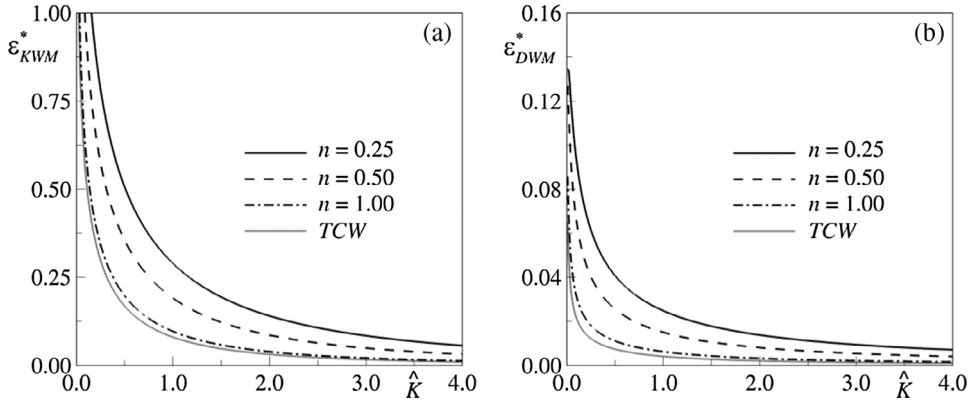

Fig. 8. Spatial distribution of the averaged relative error ($F_N = 0.1$). (a) KWM; (b) DWM.

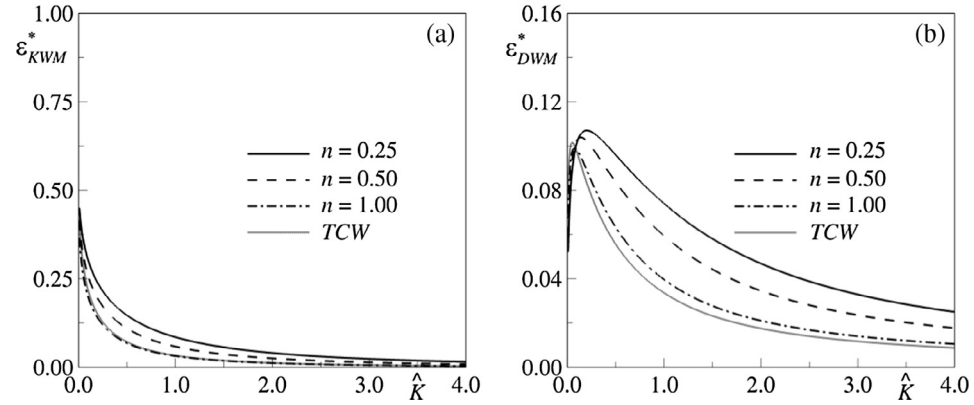

Fig. 9. Spatial distribution of the averaged relative error ($F_N = 0.5$). (a) KWM; (b) DWM.

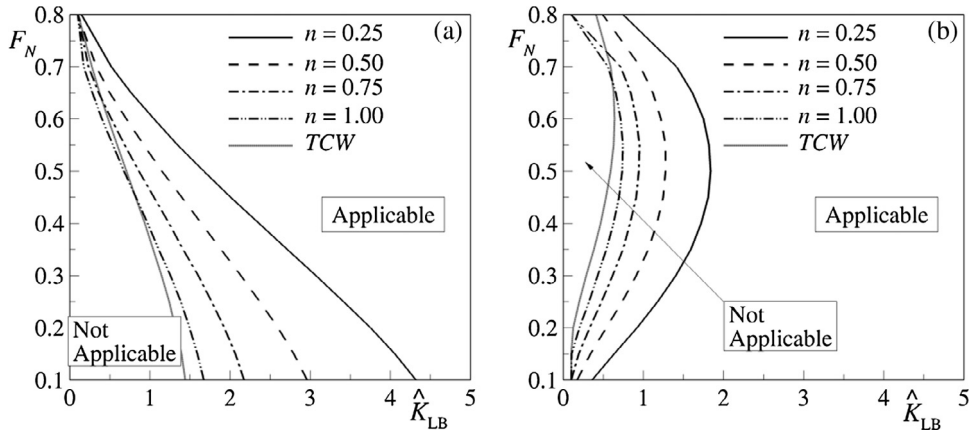

Fig. 10. Kinematic (a) and Diffusive (b) Wave Models applicability maps.

sidered as a conservative estimate of the lower bound for the applicability of the approximate models with an error less than 5%, for all subcritical Froude numbers. For the TCW flow, these threshold values are $\hat{K}_{TV}^{TCW} = 1.4$ (KWM) and $\hat{K}_{TV}^{TCW} = 0.6$ (DWM), which are in perfect agreement with those deduced by Moramarco et al. (2008a). Figure 11 reports, for both DWM and KWM, the threshold values $\hat{K}_{TV}$ obtained for several rheological exponents (black lines), which define, for each fluid, the limiting $\hat{K}$ value above which the approximated models can be safely applied. For the sake of comparison, also the corresponding ones for the TCW case ($\hat{K}_{TV}^{TCW}$ with grey color) are reported. It can be observed that the DWM has a larger applicability range than the KWM.

Figure 11 demonstrates that in presence of huge quantities of sediments, which may lend the mixture a shear-thinning power-law rheology, the applicability criteria deduced for clear-water may lead to an incorrect use of both approximated wave models. Results reported in Fig. 11 constitute a criterion for the correct application of the KWM and DWM

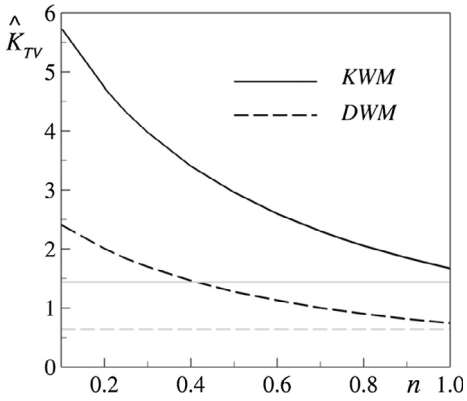

Fig. 11. Minimum values of the threshold value $\hat{K}_{TV}$ for the application of KWM and DWM. Black lines: power-law fluid, Grey lines: TCW.

models for mud-flows, extending to power-law fluids the results available in the literature for turbulent clear-water flows.

5. Conclusions

The paper investigated the applicability of the Kinematic and Diffusive Wave Models for flows of shear-thinning fluids described by a power-law rheology. The study represents an extension to the power-law rheology of the steady state analyses previously developed for turbulent clear-water (TCW) flows.

The procedure is based on the evaluation of the error associated to the application of the approximated models, accounting for the non-linearity of the governing equations. The analysis is carried out starting from the analytical solution of the flow depth profiles of both Full and Approximated models, in an infinitely wide channel under steady state conditions of flow. Similarly to the turbulent clear-water case, accelerated hypocritical flows in mild slope channel, with free-flow outlet condition, have been investigated.

It has been found that, in presence of a power-law fluid, the spatial distribution of the error for both approximated models differs with respect to that of TCW flows, revealing the important role of the rheology on the model selection. The overall analysis of the accuracy of the approximated models has been carried out considering the magnitude of the average error along the channel length for different rheological exponents and governing dimensionless numbers. Assuming a threshold on the average error of 5%, for a fixed value of the power-law index, it has been individuated a limit value of the kinematic wave number $\hat{K}_{TV}$, above which the approximate models are applicable, for all the subcritical Froude number values. Present results show that the applicability range of the Diffusive Wave model is larger than that of the Kinematic model and in both cases it decreases when n reduces. Moreover, these applicability ranges, especially for fluids with a pronounced shear-thinning attitude, strongly differ from the corresponding ones for the turbulent clear-water case. In conclusion, present study reveals that the results available in the literature for clear-water flows may not be valid for power-law fluids, and it provides novel specific applicability criteria for this class of fluids. In a future research, the present analysis will be extended considering different power-law rheologies, such as the one proposed by Lanzoni et al. (2017) for debris flows in drained inertial range. Moreover, for addressing problems with realistic mountain topographies, often associated to natural avalanches and debris flows, the analysis could be performed adopting depth-averaged models able to include the bottom curvature effect, such as, for instance, Ionescu (2013a,b) or Fent et al. (2018).

Appendix A.

Let us consider a two-dimensional laminar flow of a thin layer of mud down a plane inclined of θ with respect to the horizontal plane. Let be the $\tilde{x}$ -axis along and the $\tilde{z}$ -axis normal to the plane bed. Denoting with $\tilde{u}_x$ and $\tilde{u}_z$ the dimensional longitudinal and transverse velocity components, with $\tilde{p}$ the dimensional pressure and with $\tilde{h}$ the dimensional depth normal to the bed, the long-wave expansion of the equations of motion are the following (Ng and Mei, 1994):

$$\frac{\partial \tilde{u}_x}{\partial \tilde{x}} + \frac{\partial \tilde{u}_z}{\partial \tilde{z}} = 0 \tag{A.1}$$

$$\frac{\partial \tilde{u}_x}{\partial \tilde{t}} + \tilde{u}_x \frac{\partial \tilde{u}_x}{\partial \tilde{x}} + \tilde{u}_z \frac{\partial \tilde{u}_x}{\partial \tilde{z}} + \frac{1}{\rho}\frac{\partial \tilde{p}}{\partial \tilde{x}} = g \sin\theta + \frac{1}{\rho}\frac{\partial \tilde{\tau}_{xz}}{\partial \tilde{z}} = 0 \tag{A.2}$$

$$\frac{1}{\rho}\frac{\partial \tilde{u}_z}{\partial \tilde{z}} + g\cos\theta = 0 \tag{A.3}$$

The following boundary conditions hold:

$$\tilde{u}_x = \tilde{u}_z = 0 \quad \text{at} \quad \tilde{z} = 0 \tag{A.4}$$

$$\tilde{u}_z = \frac{\partial \tilde{h}}{\partial \tilde{t}} + \tilde{u}_x \frac{\partial \tilde{h}}{\partial \tilde{x}} \quad \text{at} \quad \tilde{z} = \tilde{h} \tag{A.5}$$

$$\frac{\partial \tilde{u}_x}{\partial \tilde{z}} = p = 0 \quad \text{at} \quad \tilde{z} = \tilde{h} \tag{A.6}$$

For a power-law fluid, the following shear stress relation is considered (Ng and Mei,1994):

$$\tilde{\tau}_{xz} = \mu_n \left|\frac{\partial \tilde{u}_x}{\partial \tilde{z}}\right|^{n-1} \frac{\partial \tilde{u}_x}{\partial \tilde{z}} \tag{A.7}$$

It is easy to verify that in uniform flow conditions only the streamwise component of the velocity is different from zero and for a power-law fluid it reads:

$$\tilde{u}_x = \frac{1+2n}{1+n}\tilde{u}\left[1 - \left(1 - \frac{\tilde{z}}{\tilde{h}}\right)^{\frac{n+1}{n}}\right] \tag{A.8}$$

Assuming that Eq. (A.8), strictly valid in uniform condition, holds even in a transient and non-uniform flow, but with $\tilde{h}$ dependent on $\tilde{x}$ and $\tilde{t}$, Eqs. (1) and (2) are obtained integrating Eqs. (A.1)-(A.3) over the film thickness, applying the Leibniz rule and accounting for the boundary conditions (A.4)-(A.6) along with (A.7).

The expression of the bottom stress τ_b in Eq. (4) is deduced from Eq. (A.7), evaluated at $\tilde{z} = 0$, accounting for (A.8). The expression (3) of the flux correction factor β straightforwardly follows from its definition:

$$\beta = \frac{1}{\tilde{h}\tilde{u}^2}\int_0^{\tilde{h}} \tilde{u}_x^2 d\tilde{z} \tag{A.9}$$

taking into account the velocity profile (A.8).

Appendix B.

This appendix illustrates the derivation of Eq. (21) from Eq. (16) for $n = 1/2$. For this power-law exponent value, it results $w = 1/2$ and Eq. (16) can be therefore rewritten as:

$$-\frac{1}{2KF_N^2}\left[\int \frac{\sqrt{\xi}}{1-\xi}d\xi - \beta F_N^2 \int \frac{1}{\xi(1-\xi)}d\xi\right] \tag{B.1}$$

Assuming $\eta = \sqrt{\xi}$, it results $d\xi = 2\eta d\eta$ and the first integral can be rewritten and solved:

$$\int \frac{\sqrt{\xi}}{1-\xi} d\xi = -2 \int \frac{\eta^2}{(\eta^2-1)} d\eta = -2\eta - \ln \frac{\eta-1}{\eta+1} \tag{B.2}$$

In terms of the ξ variable, the solution is:

$$\int \frac{\sqrt{\xi}}{1-\xi} d\xi = -2\sqrt{\xi} - \ln \frac{\sqrt{\xi}-1}{\sqrt{\xi}+1} \tag{B.3}$$

Concerning the second integral in Eq. (B.1), it is easily solved as:

$$\int \left(\frac{1}{\xi} + \frac{1}{1-\xi}\right) d\xi = \ln \xi - \ln(\xi - 1) \tag{B.4}$$

Finally, the solution of Eq. (B.1) is:

$$\frac{1}{KF_N^2}\left[\sqrt{\xi} + \frac{1}{2}\ln\frac{\sqrt{\xi}-1}{\sqrt{\xi}+1} - \frac{\beta F_N^2}{2}(\ln \xi - \ln(\xi-1))\right] \tag{B.5}$$

Being $\xi = h^2$ (Eq. (17)), for hypocritical currents imposing at $x = 0$ a known depth (h_*), the flow depth profile for $-1 \leqslant x_{FM} \leqslant 0$, may be deduced from Eq. (B.5), obtaining

$$x_{FM} = \frac{1}{KF_N^2}\left[h - h_* + \frac{1-\beta F_N^2}{2}\ln\left(\frac{h-1}{h_*-1}\right) - \frac{1+\beta F_N^2}{2}\ln\left(\frac{h+1}{h_*+1}\right) + \beta F_N^2 \ln\left(\frac{h}{h_*}\right)\right] \tag{B.6}$$

References

Ancey, C., Cochard, S., 2009. The dam-break problem for Herschel-Bulkey viscoplastic fluids down steep flumes. J. Non-Newtonian Fluids Mech. 158, 18–35. https://doi.org/10.1016/j.jnnfm.2008.08.008.

Ancey, C., Andreini, N., Epely-Chauvin, G., 2012. Viscoplastic dambreak waves: review of simple computational approaches and comparison with experiments. Adv. Water Resour. 48, 79–91. https://doi.org/10.1016/j.advwatres.2012.03.015.

Aricò, C., Sinagra, M., Begnudelli, L., Tucciarelli, T., 2011. MAST-2D diffusive model for flood prediction on domains with triangular Delaunay unstructured meshes. Adv. Water Resour. 34, 1427–1449. https://doi.org/10.1016/j.advwatres.2011.08.002.

Aricò, C., Filianoti, P., Sinagra, M., Tucciarelli, T., 2016. The FLO diffusive 1D–2D model for simulation of river flooding. Water 8 (200). https://doi.org/10.3390/w8050200.

Arattano, M., Savage, W.Z., 1994. Modelling debris flows as kinematic waves. Bull. Int. Assoc. Eng. Geol. 49, 3–13. https://doi.org/10.1007/BF02594995.

Arattano, M., Franzi, L., 2006. L., Marchi, Influence of rheology on debris-flow simulation. Nat. Hazards Earth Syst. Sci. 6 (4), 519–528. https://doi.org/10.5194/nhess-6-519-2006.

Arattano, M., Franzi, L., 2010. On the application of kinematic models to simulate the diffusive processes of debris flows. Nat. Hazards Earth Syst. Sci. 10, 1689–1695. https://doi.org/10.5194/nhess-10-1689-2010.

Balmforth, N.J., Craster, R.V., Rust, A.C., Sassi, R., 2007. Viscoplastic flow over an inclined surface. J. Non-Newtonian Fluids Mech. 142, 219–243. https://doi.org/10.1016/j.jnnfm.2006.07.013.

Campomaggiore, F., Di Cristo, C., Iervolino, M., Vacca, A., 2016. Development of roll waves in power-law fluids with non-uniform initial conditions. J. Hydraul. Res. 54 (3), 289–306. https://doi.org/10.1080/00221686.2016.1140684.

Carotenuto, C., Merola, M.C., Ālvarez-Romero, M., Coppola, E., Minale, M., 2015. Rheology of natural slurries involved in a rapid mudflow with different soil organic carbon content. Colloids Surf. A 466, 57–65. https://doi.org/10.1016/j.colsurfa.2014.10.037.

Chiang, S.H., Chang, K.T., Mondini, A.C., Tsai, B.W., Chen, C.Y., 2012. Simulation of event-based landslides and debris flows at watershed level. Geomorphology 138, 306–318. https://doi.org/10.1016/j.geomorph.2011.09.016.

Chyan-Deng, Jan, 2014. Gradually-varied Flow Profiles in Open Channels, Analytical Solutions by Using Gaussian Hypergeometric Function. Springer, Berlin.

de Almeida, G.A.M., Bates, P., 2013. Applicability of the local inertial approximation of the shallow water equations to flood modeling. Water Resour. Res. 49, 4833–4844. https://doi.org/10.1002/wrcr.20366.

Di Cristo, C., Iervolino, M., Vacca, A., 2014a. Applicability of Kinematic, Diffusion and Quasi-Steady dynamic wave models to shallow mud flows. J. Hydrol. Eng. 19 (5), 956–965. https://doi.org/10.1061/(ASCE)HE.1943-5584.0000881.

Di Cristo, C., Iervolino, M., Vacca, A., 2014b. Simplified wave models applicability to shallow mud flows modeled as power-law fluids. J. Mountain Sci. 11 (6), 1454–1465. https://doi.org/10.1007/s11629-014-3065-6.

Di Cristo, C., Iervolino, M., Vacca, A., 2017. Wave propagation in linearized shallow flows of power-law fluids. Adv. Water Resour. https://doi.org/10.1016/j.advwatres.2017.06.022.

Dooge, J.C.I., Napiorkowski, J.J., Strupczewski, W.G., 1987. Properties of generalized downstream channel response. Acta Geophysica Polonica 35 (4), 405–416.

Fent, I., Putti, M., Gregoretti, C., Lanzoni, S., 2018. Modeling Shallow Water Flows on General Terrains. Adv. Water Resour. https://doi.org/10.1016/j.advwatres.2017.12.017.

Ferrick, M.G., 1985. Analysis of river wave types. Water Resour. Res. 21 (2), 209–220. https://doi.org/10.1029/WR021i002p00209.

Fread, D.L., 1983. Applicability criteria for kinematic and diffusion routing models. HRL 183, Hydrology Research Laboratory, National Weather Service, NOAA, Silver Spring, Md.

Govindaraju, R.S., Jones, S.E., Kavvas, M.L., 1988a. On the diffusion wave model for overland flow: Solution for steep slopes. Water Resour. Res. 24 (5), 734–744. https://doi.org/10.1029/WR024i005p00734.

Govindaraju, R.S., Jones, S.E., Kavvas, M.L., 1988b. On the diffusion wave model for overland flow: steady state analysis. Water Resour. Res. 24 (5), 745–754. https://doi.org/10.1029/WR024i005p00745.

Gregoretti, C., Degetto, M., Boreggio, M., 2016. GIS-based cell model for simulating debris flow runout on a fan. J. Hydrol. 534, 326–340. https://doi.org/10.1016/j.jhydrol.2015.12.054.

Honda, N., Egashira, S., 1997. Prediction of debris flow characteristics in mountain torrents. In: Proceedings of the First International ASCE Conference on Debris-Flow Hazard Mitigation: Mechanics, Prediction and Assessment, San Francisco, CA, August 7–9, pp. 707–716.

Huang, X., Garcia, M.H., 1998. A Herschel-Bulkley model for mud flow down a slope. J. Fluid Mech. 374, 305–333. https://doi.org/10.1017/S0022112098002845.

Ionescu, I.R., 2013a. Augmented Lagrangian for shallow viscoplastic flow with topography. J. Comput. Phys. 242, 544–560. https://doi.org/10.1016/j.jcp.2013.02.029.

Ionescu, I.R., 2013b. Viscoplastic shallow flow equations with topography. J. Nonnewton. Fluid Mech. 193, 116–128. https://doi.org/10.1016/j.jnnfm.2012.09.009.

Lamberti, P., Pilati, S., 1996. Flood propagation models for real-time forecasting. J. Hydrol. 175, 239–265. https://doi.org/10.1016/S0022-1694(96)80013-8.

Lanzoni, S., Gregoretti, C., Stancanelli, L., 2017. Coarse-grained debris flow dynamics on erodible beds. J. Geophys. Res. Earth Surf. 122, 592–614. 0.1002/2016JF004046.

Menendez, A.N., Norscini, R., 1982. Spectrum of shallow water waves. J. Hydraul. Div. 108 (1), 75–94.

Moramarco, T., Singh, V.P., 2000. A practical method for analysis of river waves and for kinematic wave routing in natural channel networks. Hydrol. Process. 14, 51–62. https://doi.org/10.1002/(SICI)1099-1085(200001)14:1<51::AID-HYP909>3.0.CO;2-Z.

Moramarco, T., Pandolfo, C., Singh, V.P., 2008a. Accuracy of Kinematic Wave and Diffusion Wave Approximations for Flood Routing. I: Steady Analysis. J. Hydrol. Eng. 13 (11), 1078–1088. https://doi.org/10.1061/(ASCE)1084-0699(2008)13:11(1078).

Moramarco, T., Pandolfo, C., Singh, V.P., 2008b. Accuracy of Kinematic Wave Approximations for Flood Routing. II: Unsteady Analysis. J. Hydrol. Eng. 13 (11), 1089–1096. https://doi.org/10.1061/(ASCE)1084-0699(2008) 13:11(1089).

Morris, E.M., Woolhiser, D.A., 1980. Unsteady one-dimensional flow over a plane: Partial equilibrium and recession hydrographs. Water Resour. Res. 16 (2), 355–360. https://doi.org/10.1029/WR016i002p00355.

Moussa, R., Boequillon, C., 1996. Criteria for the choice of flood routing methods in natural channels. J. Hydrol. 186, 1–30. https://doi.org/10.1016/S0022-1694(96)03045-4.

Ng, C., Mei, C.C., 1994. Roll waves on a shallow layer of mud modeled as a power-law fluid. J. Fluid Mech. 263, 151–184. https://doi.org/10.1017/S0022112094004064.

O'Brien, J.S., Julien, P.Y., Fullerton, W.T., 1993. Two-dimensional water flood and mudflow simulation. J. Hydraul. Eng. 119 (2), 244–261. https://doi.org/10.1061/(ASCE)0733-9429(1993) 119:2(244).

Parlange, J.Y., Hogarth, W., Sander, G., Rose, C., Heverkamp, R., Surin, A., Brutsaert, W., 1990. Asymptotic expansion for steady-state overland flow. Water Resour. Res. 26 (4), 579–583. https://doi.org/10.1029/WR026i004p00579.

Pudasaini, S.P., 2001. Some exact solutions for debris and avalanche flows. Phys. Fluids 23, 043301. https://doi.org/10.1063/1.3570532.

Perumal, M., Sahoo, B., 2007. Applicability criteria of the parameter Muskingum stage and discharge routing methods. Water Resour. Res. 43 (5), W05409. https://doi.org/10.1029/2006WR004909.

Ponce, V.M., Li, R.M., Simons, D.B., 1978. Applicability of kinematic and diffusion models. J. Hydraul. Div. 104 (HY3), 353–360.

Rengers, F.K., McGuire, L.A., Kean, J.W., Staley, D.M., Hobley, D.E.J., 2016. Model simulations of flood and debris flow timing in steep catchments after wildfire. Water Resour. Res. 52. https://doi.org/10.1002/2015WR018176.

Singh, V.P., Aravamuthan, Y., 1995a. Errors of kinematic-wave and diffusion-wave approximations for time-independent flows. Water Resour. Manage. 9 (3), 175–202. https://doi.org/10.1007/BF00872128.

Singh, V.P., Aravamuthan, Y., 1995b. Accuracy of kinematic-wave and diffusion-wave approximations for time-independent flows. Hydrol. Process. 9 (7), 755–782. https://doi.org/10.1002/hyp.3360090704.

Singh, V.P., Aravamuthan, Y., 1996. Errors of kinematic-wave and diffusion-wave approximations for steady-state overland flows. CATENA 27 (3–4), 209–227. https://doi.org/10.1016/0341-8162(96)00021-5.

Singh, V.P., 1996. Errors of kinematic-wave and diffusion-wave approximations for space-independent flows on infiltrating surfaces. Hydrol. Process. 10 (7),

955–969. https://doi.org/10.1002/(SICI)1099-1085(199607)10:7<955::AID-HYP350>3.0.CO;2-G.
Singh, V.P., Aravamuthan, V., 1997. Accuracy of kinematic wave and diffusion wave approximations for time-independent flows with momentum exchange included. Hydrol. Process. 11 (5), 511–532. https://doi.org/10.1002/(SICI)1099-1085(199704)11:5<511::AID-HYP444>3.0.CO;2-Z.
Tsai, C.W., 2003. Applicability of kinematic, noninertia, and quasisteady dynamic wave models to unsteady flow routing. J. Hydraul. Eng. 129 (8), 613–627. https://doi.org/10.1061/(ASCE)0733-9429(2003) 129:8(613).
Weill, S., Chiara-Roupert, R., Ackerer, P., 2014. Accuracy and deficiency of time integration methods for 1D diffusive wave equation. Comput. Geosci. 18, 697–709. https://doi.org/10.1007/s10596-014-9417-z.
Weisstein, E.W., 1998. CRC Concise Encyclopedia of Mathematics. CRC Press, Boca Raton, FL.
Woolhiser, D.A., Liggett, J.A., 1967. Unsteady, one-dimensional flow over a plane: the rising hydrograph. Water Resour. Res. 3 (3), 753–771. https://doi.org/10.1029/WR003i003p00753.
Yu, D., Lane, N., 2006. Urban fluvial flood modelling using a two-dimensional diffusion-wave treatment, part 1: mesh resolution effect. Hydrol. Process. 20, 1541–1565. https://doi.org/10.1002/hyp.5935.
Zhang, X., Bai, Y., and Ng, C.O., 2010. Rheological Properties of Some Marine Muds Dredged from China Coasts. In: Proceedings of the 28 International Offshore and Polar Engineering Conference, Beijing, China, pp. 455–461.